Iranian Journal of Hydrogen & Fuel Cell 4(2017) 275-287

Iranian Journal of Hydrogen & Fuel Cell

IJHFC

Journal homepage://ijhfc.irost.ir

Energy and economic comparison of SOFC-GT, MCFC-GT, and SOFC-MCFC-GT hybrid systems

Saber Sadeghi *

Department of Mechanical Engineering, Graduate University of Advanced Technology, Kerman, Iran.

Article Information

Article History:

Received:
06 Jan 2018
Received in revised form:
15 Feb 2018
Accepted:
27 Feb 2018

Keywords

SOFC
MCFC
hybrid system
energy analysis
economic analysis

Abstract

Conversion of fossil fuels to electrical power is the most popular method of electrical power generation. Due to the depletion of fossil fuels and the increase in air pollution, the necessity of using high efficiency power generation systems is increasing. High temperature fuel cells, such as solid oxide fuel cells (SOFC) and molten carbonate fuel cells (MCFC), have high efficiency. According to the high operation temperature of these fuel cells, there is the possibility of combining of them with gas turbines (GT) to reach to a higher efficiency. In the present study, the SOFC-GT hybrid system, the MCFC-GT hybrid system, and the new SOFC-MCFC-GT hybrid system are compared from an energy and economic point of view. The results show that the MCFC-GT has the highest efficiency but its annualized cost is greater than the others. The new SOFC-MCFC-GT hybrid system is more efficient than the SOFC-GT hybrid system for low current density, high fuel utilization, and high air utilization. This new hybrid system has lower annualized cost than MCFC-GT hybrid system.

1. Introduction

From an environmental point of view, it is interested to use a high energy efficiency system, such as fuel cells, to generate electrical power. Some of the fuel cells work at a high temperature and their output has high energy quality. Therefore, their output has the possibility to generate more power in a gas

*Corresponding Author's Fax: +98 3433776617
E-mail address:S.Sadeghi@kgut.ac.ir

doi: 10.22104/ijhfc.2018.2708.1163

turbine. Hybrid systems including high temperature fuel cells and gas turbine are currently the focus of many researchers. One of these hybrid systems, the SOFC-GT, can be considered from a different point of view. Ameri and Mohammadi [1] simulated an atmospheric SOFC and GT hybrid system by utilizing Aspen Plus functions and unit operation modules. In this study a sensitivity analysis was done for a 300kW SOFC and GT hybrid and it explained the reasons for increase or decrease of the major design parameters. Dang et al. [2] developed a numerical model for the performance analysis of solid oxide fuel cell /micro gas turbine hybrid systems with prereforming of natural gas, in which a quasi two-dimensional model has been built to simulate the cell electrochemical reaction, heat, and mass transfer within a tubular SOFC. The effects of turbine inlet temperature (TIT) and pressure ratio (PR) on the performance of the hybrid system was investigated. Massardo and Magistri [3] investigated the performance of an internal reforming solid oxide fuel cell and gas turbine combined cycles. An exergy and a thermo-economic analysis of the cycles was carried out and presented the influence of several parameters such as external reformer operating conditions, fuel-to-air ratio, cell current density, compressor pressure ratio, etc. Sreeramulu and Gupta [4] carried out a thermodynamic analysis of a SOFC-GT combined system (3MW) for the fuel methane to evaluate the energy efficiency, exergy efficiency and exergy destruction of each component and compared it with other fuels like coal gas and ethanol. They analysed the effect of compression ratio, turbine inlet temperature, and ambient temperature of air on the performance of the system. Fatahian et al. [5] simulated fuel cell compression ratios of 4, 4.1 and 4.2 at an ambient temperature of 298 K and ultimately selected an optimum ratio of 4.1 for modeling. Khani et al. [6] proposed a heat and power cogeneration system known as the SOFC-GT indirect thermal coupling scheme and identify the best practical operating condition essential to obtain the most thermodynamic and economic effective performance of the system subjected to necessary constraints through multi-objective optimization. Arsalis [7] investigated the design and performance characteristics of hybrid system configurations consisting of a SOFC, gas turbine, and steam turbine for stationary power applications, which provide power to a large number of residential/commercial buildings. Eveloy et al. [8] investigated a triple SOFC-Brayton-organic Rankine cycle to enhance power generation capacity and efficiency in a process plant. Shirazi et al. [9] modeled an internal-reforming solid oxide fuel cell-gas turbine hybrid system and analyzed it from thermal (energy and exergy), economic, and environmental points of view. They performeda multi-objective optimization of the system in order to achieve optimal design parameters.

Another hybrid system, the MCFC-GT, has recently caught the attention of researchers. Haghighat Mamaghani et al. [10] modeled a molten carbonate fuel cell-gas turbine hybrid plant from energetic, exergetic, economic and environmental standpoints and optimized the system through a multi-objective optimization scheme. They employed the TOPSIS decision-making method to determine the system final optimum design, leading to an overall exergetic efficiency of 51.7% and a total cost of 0.324 million USD per year. Zhang et al. [11] established a model of the molten carbonate fuel cell and gas turbine hybrid system with direct internal reforming where the fuel cell and the auxiliary burner were taken as the heat reservoirs of the GT. They found that the efficiency of the hybrid system increases by adding the utilization factor of the hydrogen, and the maximum power output of the hybrid system is achieved when the utilization factor of the hydrogen is equal to 0.78. Haghighat Mamaghani et al. [12] proposed a hybrid system integrating high temperature MCFC-GT and ORC (organic Rankine cycle), which provides the possibility to achieve high electrical and exergetic efficiencies owing to the subsequent electrical power output in the bottoming cycle. El-Emam and Dincer [13] performed energy and exergy analyses and an efficiency assessment for a biogas fueled MCFC combined with gas turbine system.

In the present study, a new hybrid system including SOFC, MCFC, and GT is investigated. This new hybrid system is compared with the SOFC-GT and MCFC-GT hybrid systems from energy and economic standpoints. The effect of changes in different parameters (current density, fuel utilization, and air utilization) are considered on the efficiency, annualized cost, power, voltage and temperature of the fuel cells.

2.Mathematical modeling

2.1. Solid oxide fuel cell

The solid oxide fuel cell used in this study is a type of tubular solid oxide fuel cell with internal reforming [14]. Reforming is needed to convert the fuel into hydrogen in a solid oxide fuel cell fed by a conventional fuel like natural gas. As reforming is done inside the cell, it is assumed that the mechanism of reactions taking place inside the cell is as follows:

Steam reforming $x \rightarrow \left[CH_4 + H_2O \rightarrow CO + 3H_2\right]$ (1)

Water gas Shifting $y \rightarrow \left[CO + H_2O \rightarrow CO_2 + H_2\right]$ (2)

Electrochemical reaction $z \rightarrow \left[H_2 + \frac{1}{2}O_2 \rightarrow H_2O\right]$ (3)

The hydrogen produced by reforming and shifting reactions with the available oxygen in the air participates in the electrochemical reaction. In the above relations, x, y, and z are the molar rates of reaction progress for steam reforming, water-gas shifting, and electrochemical reactions, respectively. As the reforming and shifting reactions are in equilibrium state, the equilibrium constants of the reactions can be calculated according to equations (4-7).

$$K_{p,r} = \frac{P_{H2}^3 \times P_{CO}}{P_{CH4} \times P_{H2O}} \quad (4)$$

$$K_{p,s} = \frac{P_{CO2} \times P_{H2}}{P_{CO} \times P_{H2O}} \quad (5)$$

$$K_{p,r} = \frac{\left(\left[\dot{n}_{H2}\right]^{in} + 3x + y - z\right)^3 \times \left(\left[\dot{n}_{CO}\right]^{in} + x - y\right)}{\left(\left[\dot{n}_{CH4}\right]^{in} - x\right) \times \left(\left[\dot{n}_{H2O}\right]^{in} - x - y + z\right)} \times \frac{P_{cell}^2}{\left(\left[\dot{n}_{tot}\right]^{in} + 2x\right)^2} \quad (6)$$

$$K_{p,r} = \frac{\left(\left[\dot{n}_{CO2}\right]^{in} + y\right) \times \left(\left[\dot{n}_{H2}\right]^{in} + 3x + y - z\right)}{\left(\left[\dot{n}_{CO}\right]^{in} + x - y\right) \times \left(\left[\dot{n}_{H2O}\right]^{in} - x - y + z\right)} \quad (7)$$

The equilibrium constants of reforming and shifting reactions are directly correlated to the temperature by a polynomial equation:

$$LogK_p = AT^4 + BT^3 + CT^2 + DT + E \quad (8)$$

where A, B, C, D, and E are the experimental constants, their values are listed by Chan [14]. The fuel utilization factor (U_f) in the anode side is defined as the ratio of reacted hydrogen to the produced hydrogen.

$$U_f = \frac{z}{3x + y} \rightarrow z = U_f \times (3x + y) \quad (9)$$

The reversible voltage of fuel cell is calculated by the Nernst equation:

$$E = E^{\circ} + \frac{R_u T}{n_e F} Ln\left(\frac{P_{H2} P_{O2}^{0.5}}{P_{H2O}}\right) \quad (10)$$

where E° is the voltage of the fuel cell in standard conditions, Ru is the universal gas constant, T is the operating temperature of the fuel cell, F is the Faraday's constant, and ne is the number of circulated electron in circuit for the formation of each water molecule. The real voltage of the fuel cell is less than the Nernst voltage due to irreversibility in the fuel cell. This irreversibility can be divided into three groups: activation loss, ohmic loss, and concentration loss. The value of real voltage is calculated according to equation (11):

$$V_{cell} = E - \left(V_{act} + V_{ohm} + V_{conc}\right) = E - \Delta V_{Loss} \quad (11)$$

The value of activation losses is equal to the sum of activation losses of the anode and cathode, and will be obtained by simplifying the Butlere-Volmers equation:

$$V_{act} = V_{act,an} + V_{act,ca} \quad (12)$$

$$V_{act} = \frac{2R_uT}{n_eF}\sinh^{-1}\left(\frac{i}{2i_{\circ,an}}\right) + \frac{2R_uT}{n_eF}\sinh^{-1}\left(\frac{i}{2i_{\circ,ca}}\right) \quad (13)$$

where i and i° are the current density and the exchange current density, respectively.

The ohmic losses are related to the transfer of electrons and ions in the anode, cathode, electrode, and internal connectors. The ohmic losses are obtained by equations (14-17):

$$V_{ohm} = V_{ohm,an} + V_{ohm,ca} + V_{ohm,el} + V_{ohm,inc} \quad (14)$$

$$V_{ohm} = ir \quad (15)$$

$$r = \delta\rho \quad (16)$$

$$\rho = Aexp\left(\frac{B}{T}\right) \quad (17)$$

The values of A, B, and δ in equations (16) and (17) are constant parameters that depend on the geometry and type of the fuel cell. The values of these parameters are listed by V. Akkaya [15].

The value of concentration losses is calculated by the following equations:

$$V_{conc} = V_{conc}^{an} + V_{conc}^{ca} \quad (18)$$

$$V_{conc}^{an} = \frac{R_uT}{n_eF}Ln\left(\frac{1 - i/i_{L,H2}}{1 + i/i_{L,H2O}}\right) \quad (19)$$

$$V_{conc}^{ca} = \frac{R_uT}{n_eF}Ln\left(\frac{1}{1 + i/i_{L,O2}}\right) \quad (20)$$

where, i_L is the limiting current density.

The power generated by SOFC can be calculated based on the real voltage of the fuel cell by equations (21-23):

$$I_{tot} = 2Fz \quad (21)$$

$$Power_{DC-tot} = V_{cell}I_{tot} \quad (22)$$

$$Power_{AC-tot} = Power_{DC-tot} \times \eta_{inv,FC} \quad (23)$$

where I_{tot} is the total current of the fuel cell and η_{invt},sofc is the coefficient of inversion of direct to alternative current in the fuel cell.

Since the reforming reaction is endothermic and the shifting reaction is exothermic, the value of heat produced from the reforming and shifting reactions are obtained by:

$$\dot{Q}_r = x\left(\overline{h}_{CO} + 3\overline{h}_{H2} - \overline{h}_{CH4} - \overline{h}_{H2O}\right) \quad (24)$$

$$\dot{Q}_{sh} = x\left(\overline{h}_{CO2} + \overline{h}_{H2} - \overline{h}_{CO} - \overline{h}_{H2O}\right) \quad (25)$$

The heat produced from electrochemical reaction is supplied from two main sources. One is due to the reversible reaction and the other is due to the voltage losses of the fuel cell. The value of the heat produced from the electrochemical reaction also is calculated as follows:

$$\dot{Q}_{elec} = zT\Delta S - I\Delta V_{Loss} \quad (26)$$

$$\Delta S = \left(S^{\circ}_{H2O} - S^{\circ}_{H2} - \frac{1}{2}S^{\circ}_{O2}\right) + \frac{R_u}{2}Ln\left(\frac{P^2_{H2} \times P_{O2}}{P^2_{H2O}}\right) \quad (27)$$

The total net heat transfer of the solid oxide fuel cell will be obtained by the difference between the heat values of the three above equations:

$$\dot{Q}_{net} = \dot{Q}_{elec} + \dot{Q}_{sh} - \dot{Q}_r \quad (28)$$

The temperature of outflow gasses from the fuel cell can be calculated by balancing the energy, and also through the use of the trial and error method.

2.2. Molten carbonate fuel cell

The electrochemical reactions at the anode and cathode of the MCFC are:

anode: $H_2 + CO_3^{2-} \rightarrow CO_2 + H_2O + 2e^-$ (29)

cathode: $\frac{1}{2}O_2 + CO_2 + 2e^- \rightarrow CO_3^{2-}$ (30)

The voltage output of fuel cells are usually affected by multi-overpotentials including the activation, ohmic, and concentration overpotentials. The species and magnitudes of overpotentials are different for different types of fuel cells. According to the semi-empirical model developed by Yuh and Selman [16, 17], the voltage output V_{cell} is given by:

$$V_{cell} = E - \left(V_a + V_c + V_{ohmic}\right) = E - \Delta V_{Loss} \quad (31)$$

where E is the ideal equilibrium potential, V_a is the anode overpotential, V_c is the cathode overpotential, and V_{ohmic} is the ohmic overpotential obtain from the following equations, respectively.

$$E = E^{\circ} + \frac{R_u T}{n_e F} Ln\left(\frac{P_{H2,a} P_{O2,c}^{0.5} P_{CO2,c}}{P_{H2O,a} P_{CO2,a}}\right) \quad (32)$$

$$V_a = 2.27\times10^{-9} iP_{H2,a}^{-0.42} P_{CO2,a}^{-0.17} P_{H2O,a}^{-1.0} \exp\left(E_{act,a} / RT\right) \quad (33)$$

$$V_c = 7.505\times10^{-10} iP_{O2,c}^{-0.43} P_{CO2,c}^{-0.09} \exp(E_{act,c} / RT) \quad (34)$$

$$V_{ohmic} = 0.5\times10^{-4} i\exp\left[3016\times\left(1/T - 1/923\right)\right] \quad (35)$$

Where E° is the ideal standard potential, R is the universal gas constant, $P_{j,a}$ is the partial pressure of constituent in the anode, $P_{j,c}$ is the partial pressure of constituent in the cathode, and E_{act} is the activation energy in the anode or cathode. The equilibrium constant of the shifting reaction can be calculated using partial pressures:

$$_{p\ r} \quad \frac{P_H \times P_{CO}}{P_{CH4} \times P_{H2O}} \quad (36)$$

$$K_{p,s} = \frac{P_{CO2} \times P_{H2}}{P_{CO} \times P_{H2O}} \quad (37)$$

The equilibrium constant of the reforming and water gas shift reaction can also be expressed in terms of the following relation:

$$LogK_{p,r} = AT^4 + BT^3 + CT^2 + DT + E \quad (38)$$

$$K_{p,s} = exp\left(\frac{4276}{T} - 3.961\right) \quad (39)$$

where A, B, C, D, and E are experimental constants, their values are listed by Chan [14].

The fuel utilization factor (U_f) in the anode side is defined as the ratio of reacted hydrogen to the produced hydrogen.

$$U_f = \frac{\dot{n}_{H2,a,in} - \dot{n}_{H2,a,out}}{\dot{n}_{H2,a,in}} \quad (40)$$

where $\dot{n}_{H2,a,in}$ is the anode hydrogen input and $\dot{n}_{H2,a,out}$ is the anode hydrogen output.

The electrical power generated by the stack is expressed as follows:

$$\dot{W}_{MCFC} = V_{cell} iA \quad (41)$$

where A is the cell area. The thermal energy generated within the MCFC stack by chemical reactions can be achieved from:

$$\dot{Q}_{elec} = zT\Delta S - I\Delta V_{Loss} \quad (42)$$

$$\Delta S = \left(S_{H2O}^{\circ} - S_{H2}^{\circ} - \frac{1}{2} S_{O2}^{\circ}\right) + \frac{R_u}{2} Ln\left(\frac{P_{H2}^2 \times P_{O2}}{P_{H2O}^2}\right) \quad (43)$$

The total net heat transfer of the molten carbonate fuel cell will be obtained by the difference between the heat values of three above equations:

$$\dot{Q}_{net} = \dot{Q}_{elec} + \dot{Q}_{sh} - \dot{Q}_r \quad (44)$$

The temperature of outflow gasses from the fuel cell can be calculated by solving equations (36-44) through the use of the trial and error method.

2.3. Gas turbine

By knowing the turbine inlet temperature, pressure ratio, and the isentropic efficiency of gas turbine, the value of actual work and exhaust gas temperature can be calculated according to:

$$\frac{T_{out,s}}{T_{in}} = \left(\frac{P_{out}}{P_{in}}\right)^{\frac{k-1}{k}} \quad (45)$$

$$\eta_{GT} = \frac{w_{GT}}{w_{GT,s}} = \frac{\bar{h}_{out} - \bar{h}_{in}}{\bar{h}_{out,s} - \bar{h}_{in}} = \frac{T_{out} - T_{in}}{T_{out,s} - T_{in}} \quad (46)$$

$$\dot{W}_{GT} = \dot{n} \times \left(\bar{h}_{out} - \bar{h}_{in}\right) \quad (47)$$

2.4. Efficiency

Considering the total hybrid system as a control volume, the electrical efficiency and net output power are obtained by the following equations:

$$\eta_{elec} = \frac{\dot{W}_{net}}{\dot{n}_{fuel} \times LHV} \quad (48)$$

$$\dot{W}_{net} = \sum \dot{W}_{generate} - \sum \dot{W}_{consume} \quad (49)$$

2.5. Annualized cost

In finance, the annualized cost is the cost per year of owning and operating an asset over its entire lifespan. Annualized cost is used in the present study to compare different configurations of economic aspects. In order to calculate ANC, annualized initial capital cost, annualized operating cost, and annualized maintenance cost will be added [18]. Since the life of different components are were equal, replacement costs are not considered.

Annualized initial capital cost:

$$C_{acap} = C_{cap}.CRF(i, R_{proj}) \quad (50)$$

where C_{acap}, C_{cap}, CRF, i, and R_{proj} are the annualized initial capital cost, initial capital cost, capital recovery factor, real interest rate, and system lifespan, respectively.

Real interest rate: $i = \frac{i' - f}{f + 1}$ (51)

where i' and f are the nominal interest rate and inflation of 0.2 and 0.15, respectively.

Capital recovery factor:

$$CFR(i, R_{proj}) = \frac{i(1+i)^{R_{proj}}}{(1+i)^{R_{proj}} - 1} \quad (52)$$

The equations provided in Arsalis [7] and Haghighat Mamaghani et al. [10] are used to estimate initial capital cost, maintenance cost, and operating cost of the hybrid systems components.

3.Results

Supply of the power needed in high efficiency systems is one of the scientist's priorities. The combination of a high temperature fuel cell with a gas turbine generates a high efficiency hybrid system. Solid oxide fuel cells and molten carbonate fuel cells work at high operating temperatures: therefore, the combination of these fuel cells with a gas turbine can give high efficiency. The SOFC anode output has some unused fuel and the SOFC cathode output has some unused oxygen which can be used in a MCFC for generating power. Of course some fuel and air must be injected to the MCFC input to create suitable operating conditions. Finally, the MCFC output enters into a GT for even more power generation. This system is the SOFC-MCFC-GT hybrid system which we compared with SOFC-GT and MCFC-GT hybrid systems in this study. Fig.1 shows the schematics of these three hybrid systems. The effect of the current density change, the fuel utilization change, and the air utilization change are considered on the efficiency, annualized cost, electrical power, and the fuel cells operating voltage and temperature. The operating temperature of fuel cellswas obtained using the error and trial method for a solution of the energy balance and chemical kinetic equations simultaneously. First, the effect of current density change is considered. Fig.2 shows the changes of efficiency and annualized cost with changes in the current density for the hybrid systems. As can be seen in the figure, the efficiency of the three systems decreases as the current density increases. The MCFC-GT hybrid system is the most efficient. For current density lower than about 4100 A/m^2, the SOFC-MCFC-GT hybrid system has greater efficiency than the SOFC-GT hybrid system. The rate of efficiency change of the SOFC-MCFC-GT is higher than the SOFC-GT. Because of the increase in reforming reaction in the SOFC and the increase in the current density, the MCFC input fuel will decrease. Therefore, as shown in Figures 3 and 4, the MCFC temperature increase rate and the GT power increase rate are reduced, which causes an increase in the rate of efficiency change of SOFC-MCFC-GT.

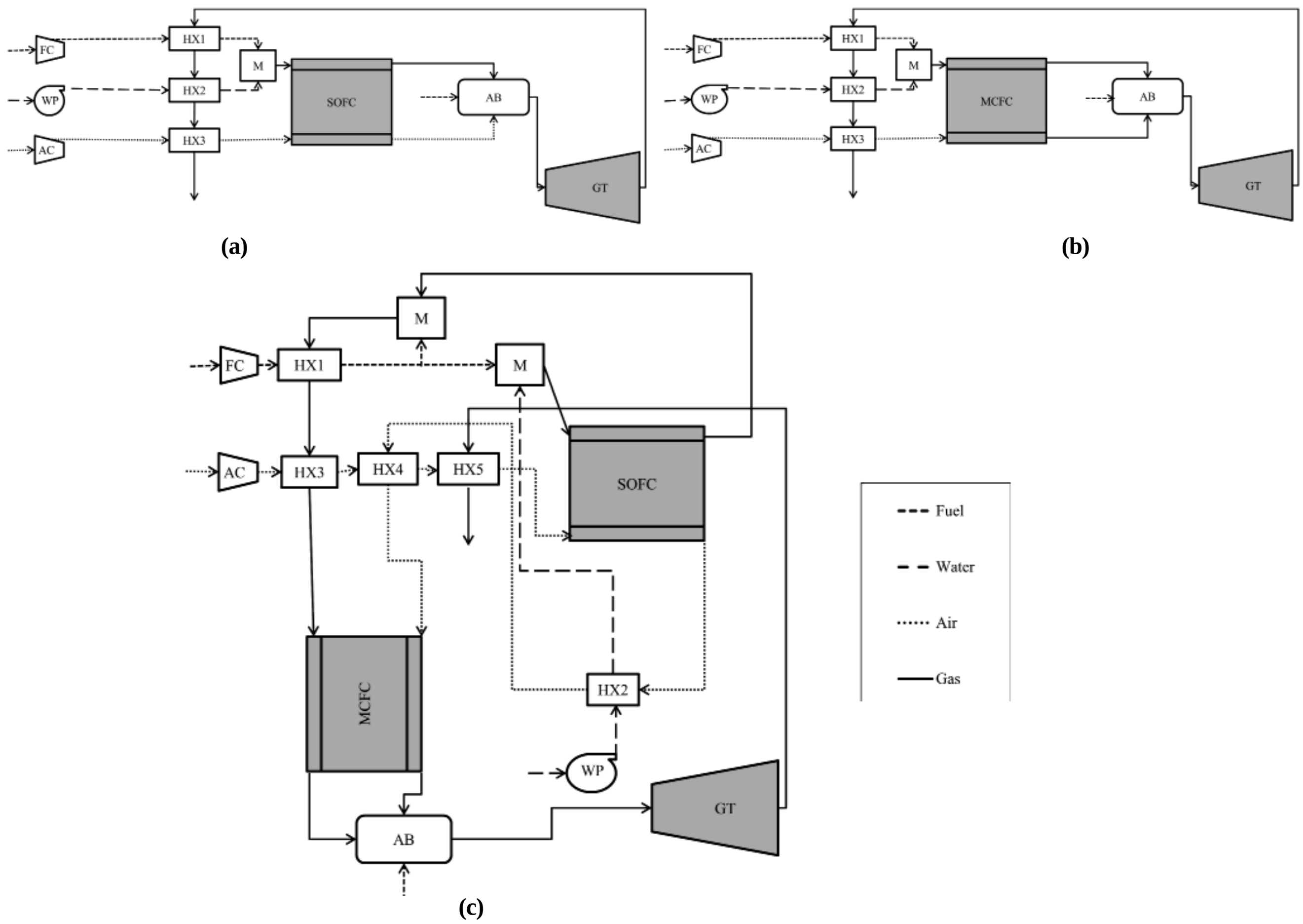

Fig. 1. Schematic of the three hybrid systems.

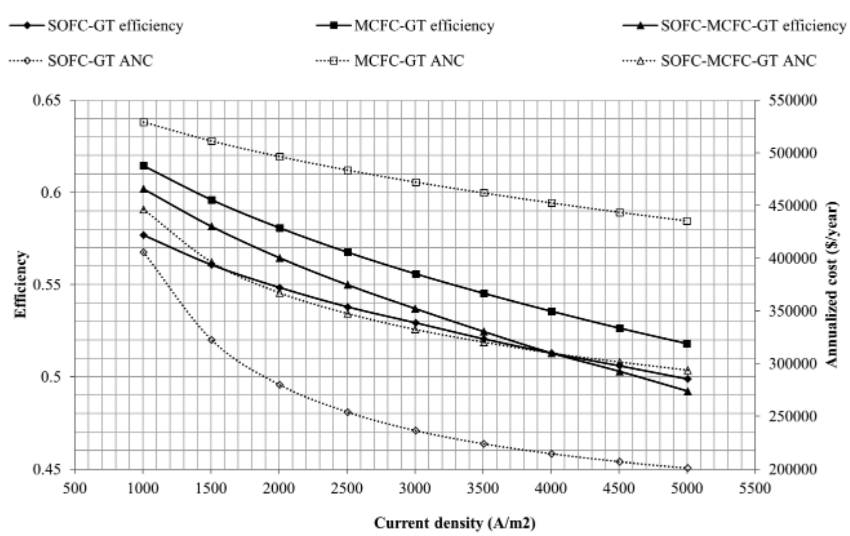

Fig. 2. Variation efficiency and annualized cost with current density.

Also, Fig.2 shows that the annualized cost of the hybrid systems decrease as the current density increases. The annualized cost of the MCFC-GT hybrid system is greater than the others. Fig.3 shows changes in the fuel cells operating voltage and temperature for the three hybrid systems with current density. Due to the same input condition for SOFC in SOFC-GT and SOFC-MCFC-GT hybrid systems, the SOFC operating voltage and temperature is exactly the same for these two hybrid systems. ’ Due

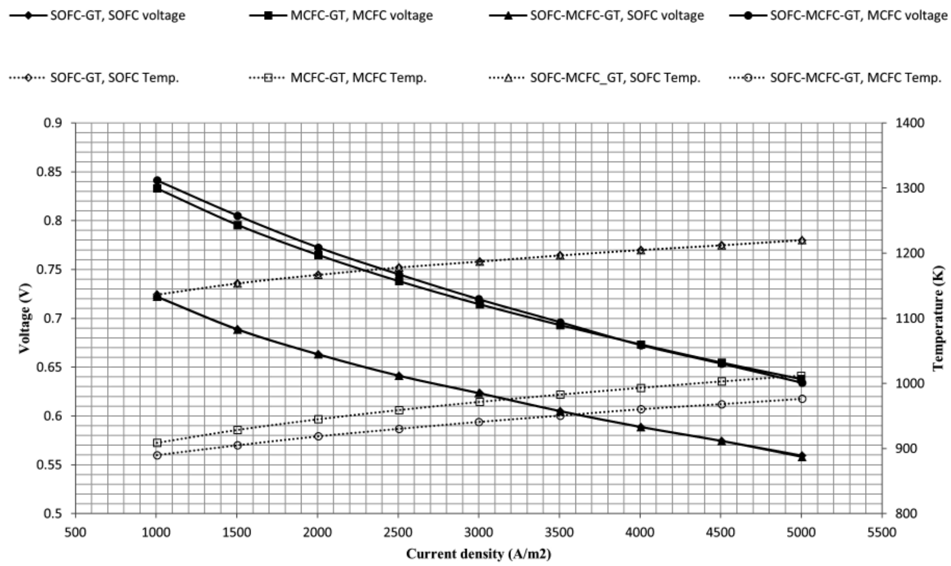

Fig. 3. Variation of fuel cell operating voltage and temperature with current density.

to different input conditions two hybrid systems.' Due to different input conditions for the MCFC, the operating voltage and temperature for MCFC-GT and SOFC-MCFC-GT hybrid systems are a little different. With the increase in current density, the fuel cells operating voltage decreases and the fuel cells operating temperature increases. Fig.4 shows the variation of total power and components' power of the hybrid systems with the change of current density. Due to a reduction of voltage with current density, the fuel cells power decreases as the current density increases. The GT power increases with current density for all three hybrid systems because of the increase in the fuel cells output temperature. The sum of the fuel cells input fuel is the same for all three hybrid systems. An injection of fuel to the after burner is needed to obtain the necessary heat for the fuel cells reactants preheating. This value as shown in Table 1 is different for the three hybrid systems. For this reason, the efficiency of the SOFC-MCFC-GT is greater than the efficiency of the SOFC-GT hybrid system.

Next, we consider the effect of fuel utilization change. An increase in the fuel utilization causes an increase in the efficiency and the annualized cost.

As shown in Fig.5, the MCFC-GT efficiency and annualized cost are greater than the other two systems. The SOFC-MCFC-GT efficiency is lower than the SOFC-GT efficiency for lower values of fuel utilization. The rate of increase in the SOFC-MCFC-GT efficiency is higher than the other two systems, and it will be greater than the SOFC-GT efficiency for higher values of fuel utilization. The reason for this is the increase in fuel consumption. This means the MCFC in the SOFC-MCFC-GT hybrid system consumes a percent of SOFC output fuel in addition to a percent of injected fuel. This causes an increase in the MCFC reactions and an increase in the MCFC power generation. Fig.6 shows changes of the fuel cells operating voltage and temperature with fuel utilization. The value of the SOFC voltage is the same for SOFC-GT and SOFC-MCFC-GT hybrid systems. It increases slowly at lower fuel utilization and decreases in fuel utilization greater than about 0.85. The MCFC operating voltage in the MCFC-GT system is greater than the SOFC voltage, but changes in the same manner as the SOFC. The MCFC voltage change in the SOFC-MCFC-GT hybrid system has a different procedure. It increases continually with the increase in fuel utilization. This is due to the increase in the H_2O partial pressure and the decrease in the H_2 partial pressure in the SOFC output as the fuel utilization increases which causes the decrease in the voltage losses according to equation (33). This figure also shows the change of fuel cells temperature with

Table 1. Fuel injected to different parts of the hybrid systems

	SOFC consumption(kmol/s)	MCFC consumption(kmol/s)	AB consumption(kmol/s)	Total consumption(kmol/s)
SOFC-GT	0.0028		0.0011	0.0039
MCFC-GT		0.0028	0.0010	0.0038
SOFC-MCFC-GT	0.0014	0.0014	0.0006	0.0034

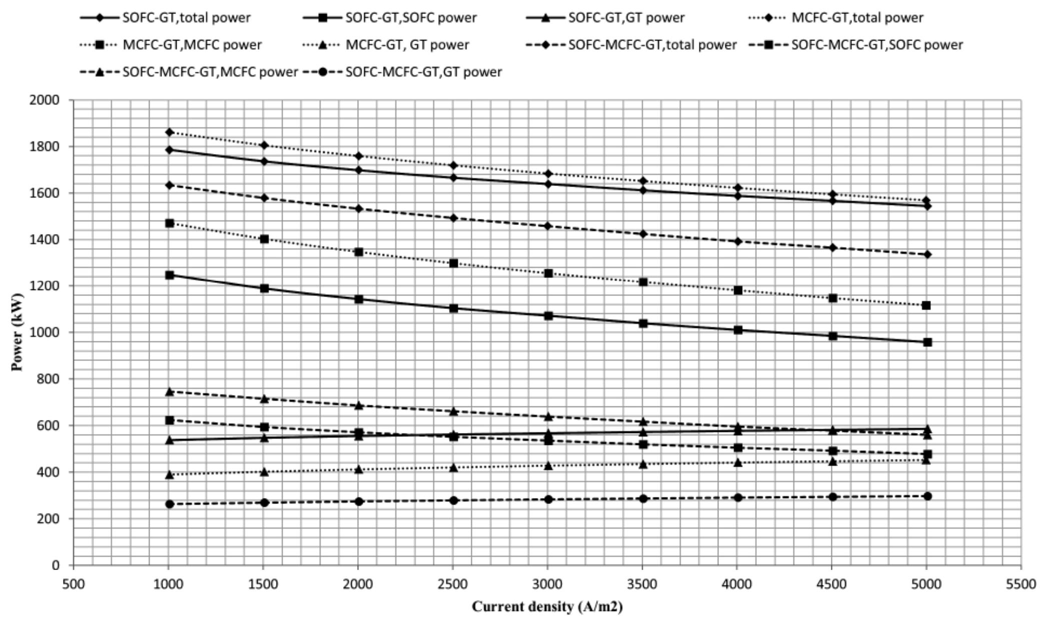

Fig. 4. Variation of total and components power with current density.

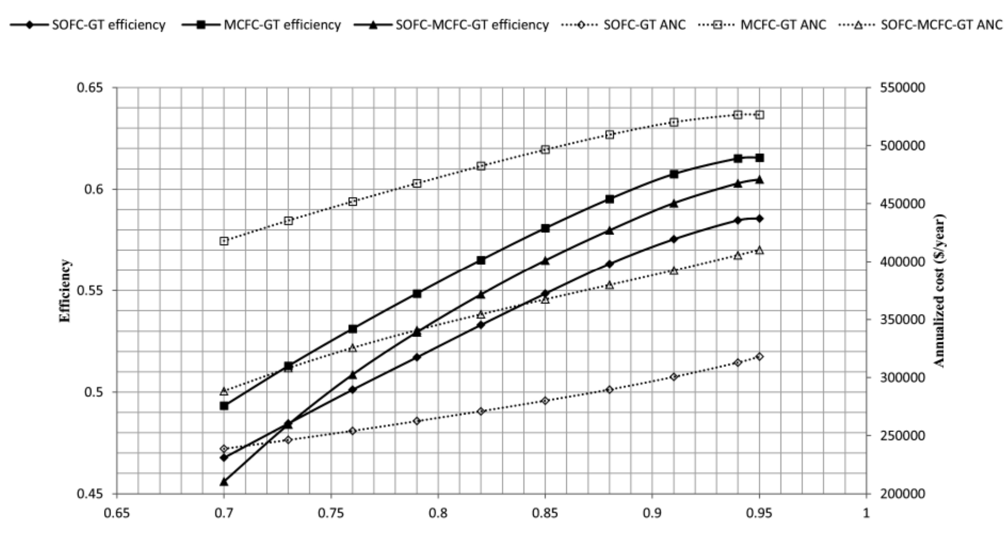

Fig. 5. Variation efficiency and annualized cost with fuel utilization.

fuel utilization. The rate of increase in the MCFC operating temperature in the SOFC-MCFC-GT hybrid system is lower than that for the other hybrid system fuel cells. Fig.7 shows the variation of total power and components' power of the hybrid systems with the change of fuel utilization. The fuel cells power increases and the GT power decreases with the increase in fuel utilization. Due to a higher portion of fuel cells power in the total power, the hybrid systems total power increases with fuel utilization. Finally, the effect of air utilization on the different parameters is considered. Fig.8 shows a small increase in the annualized cost as the air utilization increases. The efficiency of the MCFC-GT and the SOFC-MCFC-GT hybrid systems increases but the SOFC-GT efficiency decreases with air utilization. The reason is the change procedure of the GT power and its portion in the total power.

As shown in Fig.9, the GT power of the three hybrid systems decrease as the air utilization decreases. But the portion of the GT power in the total power of SOFC-GT hybrid system is greater which causes the reduction of the SOFC-GT efficiency with air utilization. Fig.10 shows the variation of the fuel

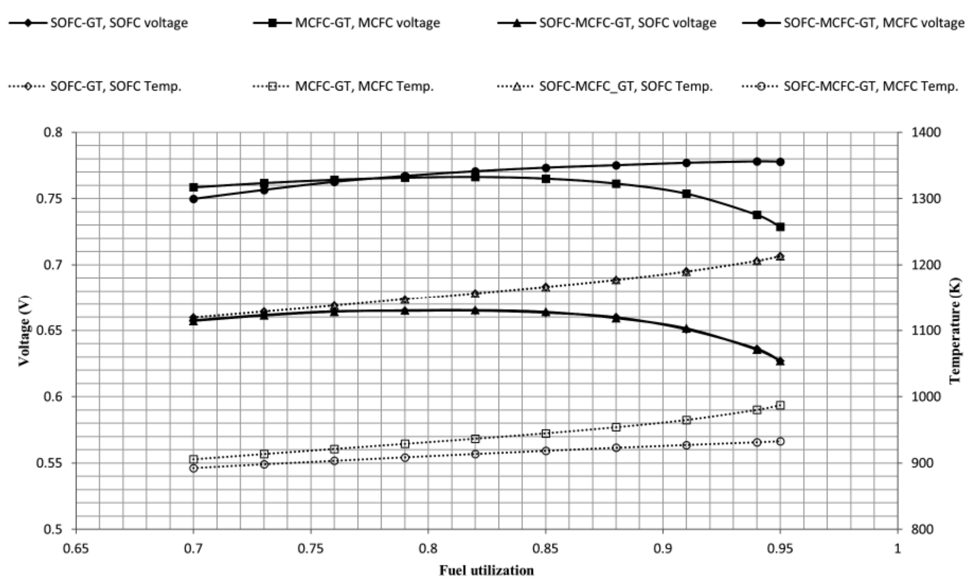

Fig. 6. Variation of fuel cell operating voltage and temperature with fuel utilization.

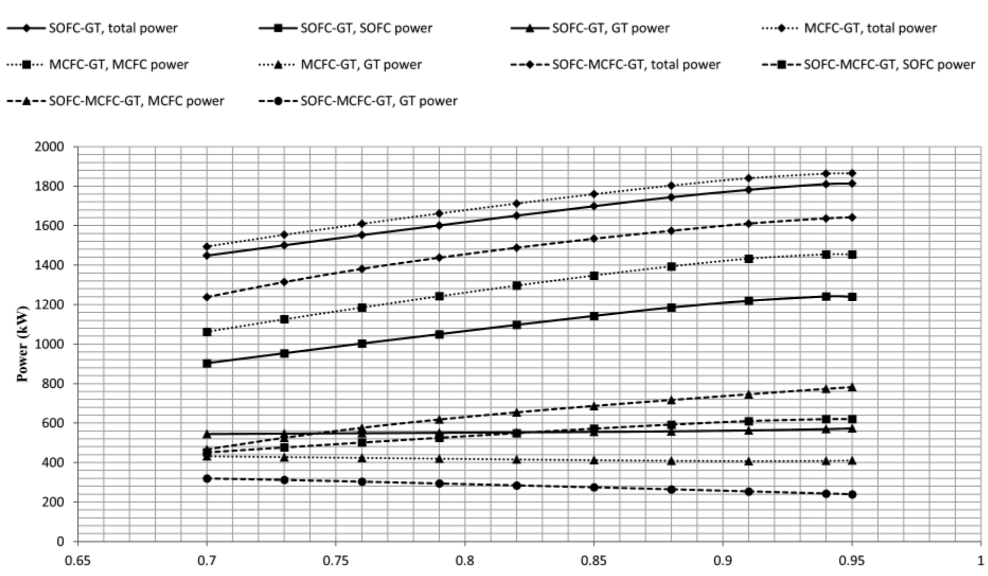

Fig. 7. Variation of total and components power with fuel utilization.

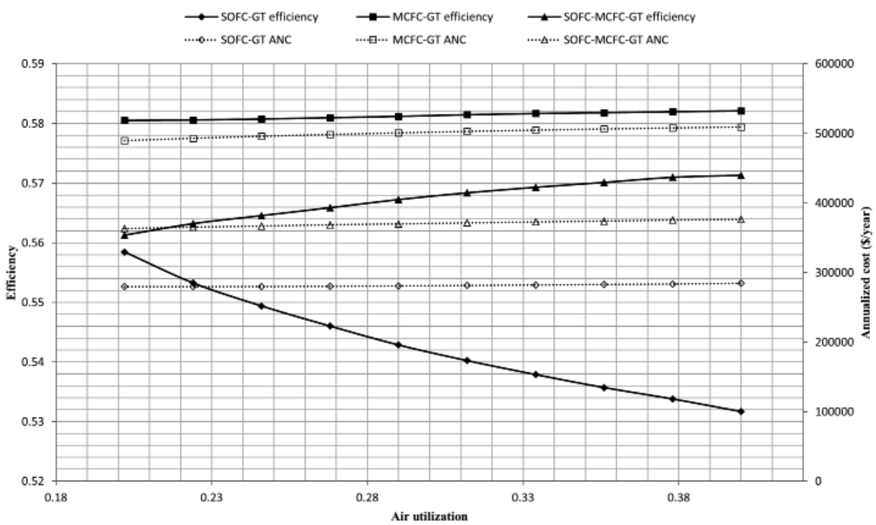

Fig. 8. Variation efficiency and annualized cost with air utilization.

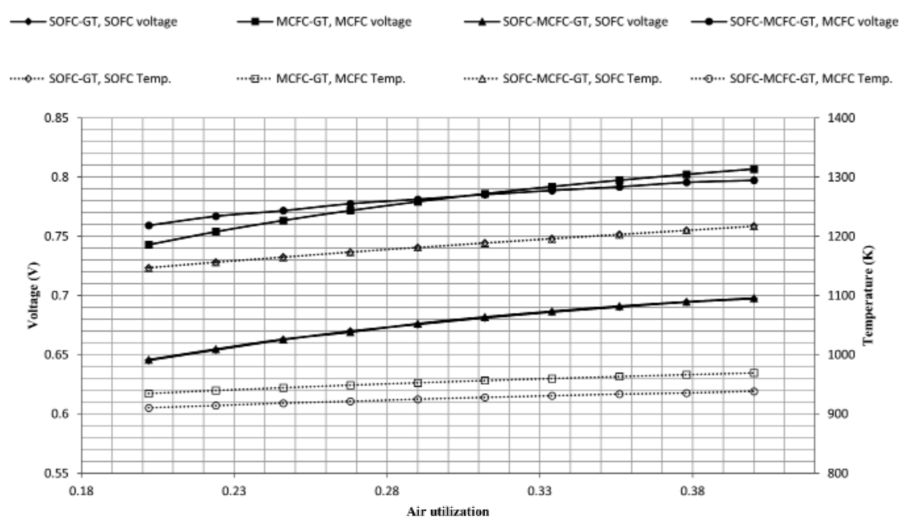

Fig. 9. Variation of total and components power with air utilization.

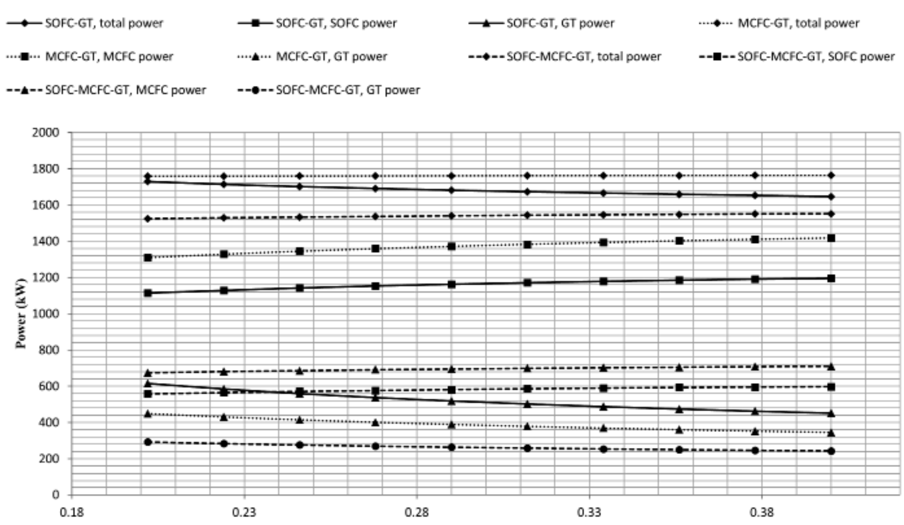

Fig. 10. Variation of fuel cell operating voltage and temperature with air utilization.

cells operating voltage and temperature. With the exception of the SOFC-GT total power and GT power of the SOFC-GT, the other components power have little change with air utilization.

4.Conclusion

In the present study, three hybrid systems (SOFC-GT, MCFC-GT, and the new SOFC-MCFC-GT) are compared from an energy and economic point of view. The effect of current density, fuel utilization, and air utilization are considered on the efficiency, annualized cost, components power, total power, voltage and temperature of the fuel cells.

The fuel cells power decreases and the GT power increases with the increase in the current density for the three hybrid systems. The fuel cells power increases and the GT power decreases with the increase in the fuel utilization. The GT power of the three hybrid systems decreases with the increase in the air utilization, but the fuel cells show different behavior. The increase in the fuel utilization causes the increase in the efficiency and the annualized cost. MCFC operating voltage in the MCFC-GT system is greater than the SOFC voltage, but it changes in the same manner. The MCFC voltage change in the SOFC-MCFC-GT hybrid system has a different changing procedure. The rate of increase in the MCFC operating temperature in SOFC-MCFC-GT hybrid system is lower than that for the other hybrid systems fuel cells. The MCFC-GT hybrid system has the greatest efficiency and unfortunately the greatest annualized cost. The SOFC-GT hybrid system has the lowest efficiency and the lowest annualized cost. The new hybrid system including SOFC, MCFC, and GT is more efficient than the SOFC-GT hybrid system for low current density, high fuel utilization, and high air utilization. The rate of increase in the SOFC-MCFC-GT efficiency with fuel utilization is higher than the other two systems. The efficiency of the MCFC-GT and the SOFC-MCFC-GT hybrid systems increases but the SOFC-GT efficiency decreases with air utilization.

Nomenclature

SOFC	Solid oxide fuel cell
MCFC	Molten carbonate fuel cell
GT	Gas turbine
AB	After burner
FC	Fuel compressor
AC	Air compressor
M	Mixer
HX	Heat exchanger
WP	Water pump

References

[1] Ameri M. and Mohammadi R., "Simulation of an atmospheric SOFC and gas turbine hybrid system using Aspen Plus software", Int. J. Energy Resources, 2011, 37:412.

[2] Dang Z., Zhao H. and Xi G., "Conceptual Design and Performance Analysis of SOFC/Micro Gas Turbine Hybrid Distributed Energy System", J. Fuel Cell Science and Technology, 2015, 12:031003/1.

[3] Massardo A. F. and Magistri L., "Internal Reforming Solid Oxide Fuel Cell Gas Turbine Combined Cycles (IRSOFC-GT)—Part II: Exergy and Thermoeconomic Analyses", J. Engineering for Gas Turbines and Power, 2003, 125:67.

[4] Sreeramulu M. and Gupta A. V. S. S. K. S., "Exergy analysis of gas turbine – solid oxide fuel cell-based combined cycle power plant", Int. J. Energy Technology and Policy, 2011, 7:469.

[5] Fatahian E., Tonekaboni N. and Fatahian H., "Exergy Analysis of Combined Cycle of Gas Turbine and Solid Oxide Fuel Cell in Different Comparison Ratios", Int. J. Scientific World 2016, 4:43.

[6] Khani L., Saberi Mehr A., Yari M. and Mahmoudi S. M. S., "Multi-objective optimization of an indirectly integrated solid oxide fuel cell-gas turbine cogeneration

system", Int. J. Hydrogen Energy, 2016, 41:21470.

[7] Arsalis A., "Thermoeconomic Modeling and Parametric Study of Hybrid Solid Oxide Fuel Cell-Gas Turbine-Steam Turbine Power Plants Ranging From 1.5 MWe to 10 MWe", J. power sources, 2008, 181:313.

[8] Eveloy V., Karunkeyoon W., Rodgers P. and Al Alili A., "Energy, exergy and economic analysis of an integrated solid oxide fuel cell-gas turbine-organic Rankine power generation system", Int. J. Hydrogen Energy, 2016, 41:13843.

[9] Shirazi A., Aminyavari M., Najafi B., Rinaldi F. and Razaghi M., "Thermal-economic-environmental analysis and multi-objective optimization of an internal-reforming solid oxide fuel cell-gas turbine hybrid system", Int. J. Hydrogen Energy, 2012, 37:19111.

[10] Haghighat Mamaghani A., Najafi B., Shirazi A. and Rinaldi F., "Exergetic, economic, and environmental evaluations and multi-objective optimization of a combined molten carbonate fuel cell-gas turbine system", Applied Thermal Engineering 2015, 77:1.

[11] Zhang X., Liu H., Ni M. and Chen J., "Performance evaluation and parametric optimum design of a syngas molten carbonate fuel cell and gas turbine hybrid system", Renewable Energy, 2015, 80:407.

[12] Haghighat Mamaghani A., Najafi B., Shirazi A. and Rinaldi F., "4E analysis and multi-objective optimization of an integrated MCFC (molten carbonate fuel cell) and ORC (organic Rankine cycle) system", Energy, 2015, 82:650.

[13] El-Emam R. S. and Dincer I., "Energy and exergy analyses of a combined molten carbonate fuel cell-Gas turbine system", Int. J. Hydrogen Energy, 2011, 36:8927.

[14] Chan S. H., Ho H. K. and Tian Y., "Modelling of simple hybrid solid oxide fuel cell and gas turbine power plant", J. Power Sources, 2002, 109:111.

[15] Volkan Akkaya A., "Electrochemical Model for Performance Analysis of a Tubular SOFC", Int. J. Energy Research, 2007, 31:79.

[16] Yuh C. Y. and Selman J. R., "The polarization of molten carbonate fuel cell electrodes: I. analysis of steady-state polarization data", J. Electrochemical Society, 1991, 138:3642.

[17] Yuh C. Y. and Selman J. R., "The polarization of molten carbonate fuel cell electrodes: II. characterization by AC impedance and response to current interruption", J. Electrochemical Society, 1991, 138:3649.

[18] Sadeghi S. and Ameri M., "Study the Combination of Photovoltaic Panels with Different Auxiliary Systems in Grid-Connected Condition", J. Solar Energy Engineering, 2014, 136:636.